Growth, spectral, optical and thermal properties of nonlinear optical sodium *para*-nitrophenolate dihydrate single crystals

S. Selvakumar and A. Leo Rajesh
Department of Physics, St. Joseph's College (Autonomous), Tiruchirappalli

1. Introduction

Nonlinear optical (NLO) materials play a vital role in fast developing fields, such as photonics and optoelectronics [1]. The organic crystals have large nonlinearity but they have poor mechanical and thermal stability [2]. Inorganic crystals have excellent mechanical and thermal properties but possess relatively modest optical nonlinearity because of the lack of extended π-electron delocalization [3]. Due to the above reason, investigations have been made on semi organic crystals which have combined properties of both organic and inorganic crystals and it is more suitable for device fabrication. The organic ligand (nitrophenoxy ion) is ionically bonded to the metal ion (inorganic host) to impart improved mechanical and thermal properties [4]. In semi-organic compounds, metal centers can act as both donors and bridging moiety in D-π-A system [5]. The metal–ligand bond is expected to display large molecular hyperpolarizablity due to the transfer of electron density between the metal atom and the conjugated ligand system [6]. Hence, investigations have been made on semi-organic crystals that have both organic and inorganic properties which is more suitable for device fabrication [7]. During the past few decades, researchers have shown much interest in the nitro phenol family of crystals due to their intensive applications in the field of opto-electronics [8]. *Para*-nitrophenol is found to be a best proton acceptor for the metallic hydroxide complexes [9]. The crystals structures of sodium *para*-nitrophenolate dihydrate single crystal were reported by Minemoto *et al* [10]. In the present work, we have report that the synthesis and growth properties of sodium paranitrophenolate dihydrate single crystal. The grown crystal is subjected to powder X-ray diffraction analysis, DRS-UV analysis, FTIR, Micro-Raman spectral studies, TG-DTA and SHG studies.

2. Experimental

2.1 Synthesis of material

The analytical grade *para*-nitrophenol and sodium hydroxide were taken in stoichiometric ratio of 1:1 and the chemical reaction is given below:

$$C_6H_5NO_3 + NaOH + H_2O \rightarrow NO_2\text{-}C_6H_4\text{-}ONa.2H_2O$$

The purity of the synthesized salt was further increased by successive recrystallization process using double distilled water. The resultant solution was completely stirred to obtain a homogenous solution and filtered using Whatman filter paper and kept it in a beaker for slow evaporation. The yellow color

crystal of dimensions with $10 \times 5 \times 2.4$ mm^3 was obtained after a period of 20 days and the photograph of the as grown crystal is shown in Figure 1.

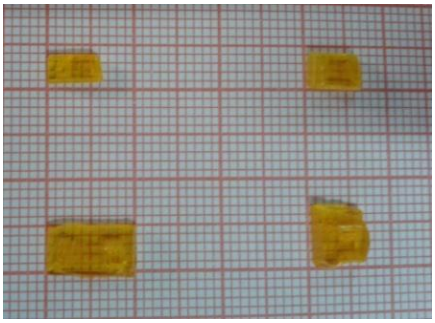

Fig. 1: Photograph of as grown NPNa crystal3. Characterization

X-ray diffraction pattern of the grown crystal was recorded by D8 Advance X-ray diffractometer with Cu Kα radiation (λ =1.5406Å) and operated at 40KV and 100 mA. The optical measurements were carried out by recording the transmission and absorbance spectra of the samples using Perkin- Elmer lambda 950, double beam UV-visible spectrophotometer. The presences of various functional groups are collected by FTIR spectrum using Bruker-Vertex 70 spectrometer. The Micro-Raman of the NPNa crystal was recorded for the wavelength region of 400-1100cm^{-1} using Jobin -Yvon Horibia (LABRAM-HR-800) spectrometer, which uses Ar^+ laser (488 nm wavelength, 10mW power) as excitation source. Thermal properties of grown crystals were studied by using the instrument SDT Q600 V20.9 BUILD 20. The second harmonic generation (SHG) efficiency test was performed by Kurtz-Perry powder technique.

4. Results and Discussion

4.1 Powder X-ray diffraction

The X-ray diffraction pattern of the sodium *para*-nitrophenolate dihydrate crystals are shown in Figure 2(a) and (b) using water and methanol respectively.

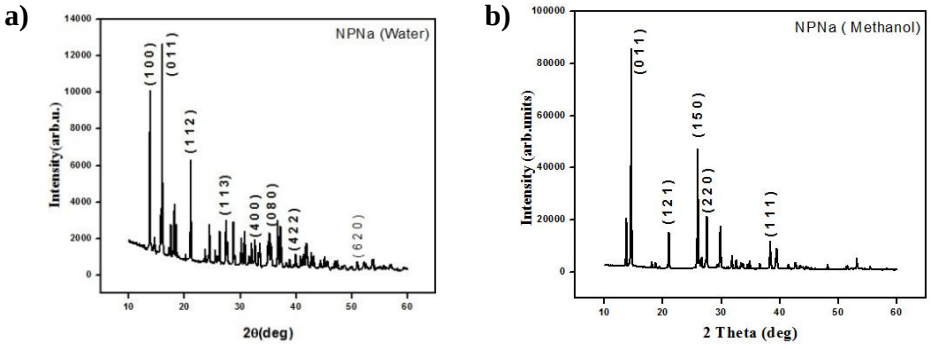

Fig. 2. Powder XRD pattern of NPNa crystals (a) Water and (b) Methanol

The sample was scanned over the 2 θ range between 10° and 60° at a scan rate of 1°/min. The 2 θ values and corresponding X-ray intensities diffracted by various planes are observed. The well-defined peaks reveal that the grown crystals are of good crystalline quality. The obtained lattice parameters that are shown in table 1 and confirms of that the grown crystals belong to orthorhombic system with the space group Ima2 and are consistent with the results reported using the single crystal X-ray diffraction. These data are in good agreement with the earlier reported data [2].

Table 1: Lattice parameter values of sodium *para*-nitrophenolate dihydrate crystal

Lattice parameter	*a* (Å)	*b* (Å)	*c* (Å)
Reported [2]	6.8920	19.6920	6.4390
Calculated (water)	6.8826	19.7249	6.4547
Calculated (Methanol)	6.8510	19.7817	6.3701

4.2 DRS –UV spectral studies

The UV analysis of grown single crystals was carried out between 200 and 2200nm using DRS-UV-Visible spectro-photometer. The absorption and transmittance spectra obtained are shown in figure 3 (a) and (b). When the absorbance is examined from longer to shorter wavelength, enhanced absorption is observed between 1400 and 2000 nm.

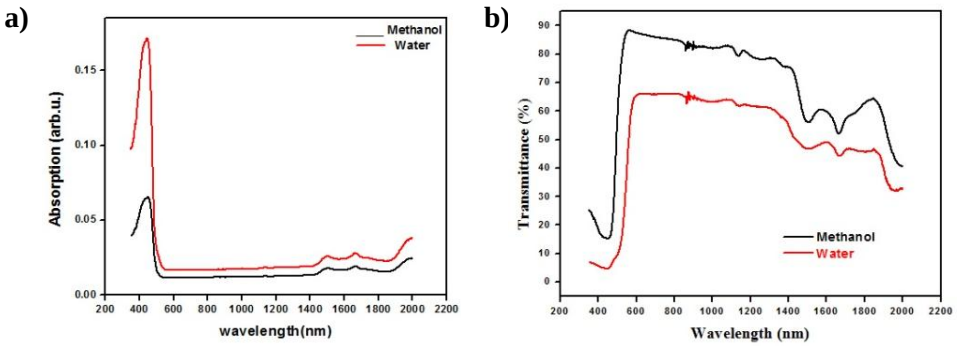

Fig. 3. The DRS-UV spectrum of NPNa crystals
(a) Absorption (b) Transmittance

The absorptions in these regions are due to overtones of some fundamental vibrations of *para*-nitrophenolate. Between the visible regions the material is observed to be highly transparent and important for crystals possessing NLO properties. The lower cut-off wavelength of the crystal in which the transmittance falls to zero is found to be at 492 nm [11].

4.3 FTIR spectral analysis

The FTIR spectrum of sodium *para*-nitrophenolate dihydrate single crystal recorded between 450 and 4000 cm^{-1} using the KBr pellet technique by a bruker, vertex 70 FTIR spectrometer and the resultant spectra are shown in Figure 4 (a) and (b) using water and methanol respectively. The broad band at 3253 and 3293cm^{-1} corresponds to O-H stretching mode of vibration respectively. The C=O stretching vibrations were absorbed at 1851cm^{-1} in both water and methanol spectrum.

The peaks at 1479 and 1470 cm^{-1} represent aromatic ring skeletal vibrations. The presence of NO_2 stretching vibration is observed at 1305cm^{-1}. The band at 844 and 854 cm^{-1} corresponds to C-H in-plane bending. The hydrate of sodium metal ion in the lattice of the crystal is found below 500 cm^{-1} [12-15].

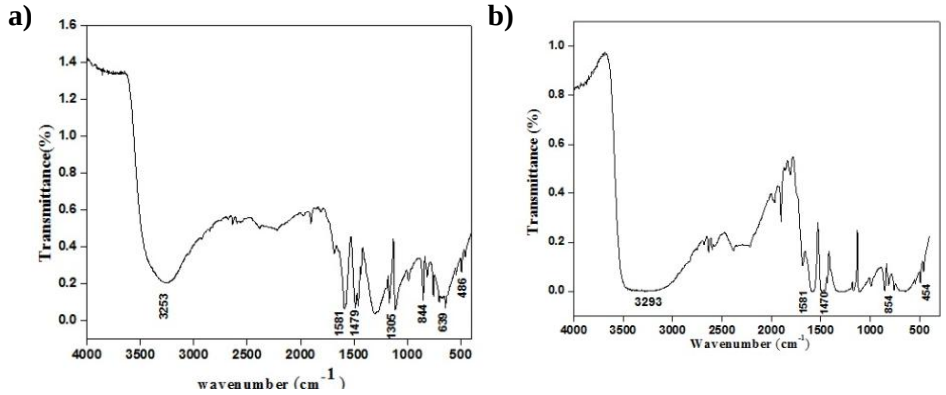

Fig. 4. FT-IR spectrum of NPNa single crystals. (a) Water (b) Methanol

4.4 Micro-Raman analysis

To confirm the various functional groups of the Micro-Raman spectrum of the grown sodium *para*-nitrophenolate dihydrate single crystal have been carried out in the wavelength region of 400-1100cm^{-1} using Jobin -Yvon Horibia (LABRAM-HR-800) spectrometer, which uses Ar^+ laser (488 nm wavelength, 10mW power) as excitation source. The room temperature Micro-Raman scattering results of NPNa single crystal is shown in Figure 5.

The observed band at 844 and 854cm^{-1} shows the C-H deformation that Benzene ring containing two adjacent H atoms. The C-OH stretching vibrations were absorbed at 1116 and 1117cm^{-1}.

The peak at 1581 and 1589cm^{-1} represents NO_2 stretching vibration. The presences of aromatic ring skeletal vibrations are observed at 1591 and 1596 cm^{-1}. The excitation wavelength of sodium atom is confirmed by the band at 390 and 395cm^{-1} [16-17].

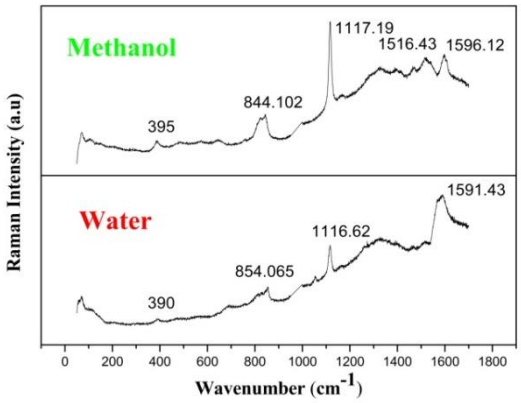

Fig. 5. Micro-Raman spectrum of NPNa single crystals

4.5 Thermal analaysis

TGA and DTA analysis of NPNa crystal was carried out between room temperature and 400 ˚C at a heating rate of 10^{o}C/minute in the nitrogen atmosphere using the instrument SDT Q600 V20.9 BUILD 20.

The respective thermogram (TG-DTA and DSC) curves are given in Figure 6.

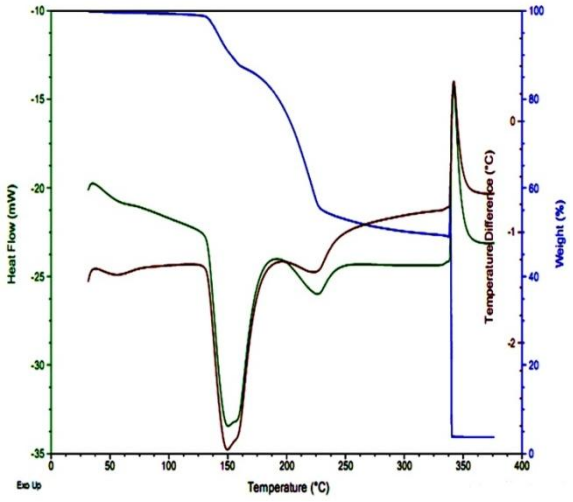

Fig. 6. TG-DTA-DSC curve of NPNa

The TGA curve of NPNa crystal reveals that there is a weight loss of 34%between 137.5 and 231.25˚C in the TGA curve coincide with the endothermic DTA peak at 150˚C. This could be attributed to the loss of lattice water. Another sharp and major weight loss of 40% occurs at 337˚C confirms the sharp exothermic peak at 338˚C indicating the complete decomposition of

the material. The thermal analysis of NPNa indicated that there is no phase transition. Hence NPNa crystal can be exploited for device fabrication between room temperature and 137˚C.

4.6 Second harmonic generation

The experiment of second harmonic generation efficiency was performed using Kurtz-Perry powder technique [18] with Nd: YAG laser source of Wavelength 1064 nm. The grown crystal of NPNa crystal was crushed to fine powder. A high intensity laser radiation was passed through the sample. The SHG was confirmed by the emission of green radiation. The intensity of the SHG output was compared with that of KDP. The SHG efficiency of NPNa crystal was 1.2 times that of KTP.

5. Conclusion

Good optical quality crystal of sodium *para*-nitrophenolate dihydrate having dimensions of $10 \times 5 \times 2.4$ mm^3 have been grown successfully with in a period of 20 days by slow evaporation technique. Lattice parameters were evaluated by powder X-ray diffraction technique which has confirmed that the grown crystal belongs to the orthorhombic crystal with space group Ima2. The optical study shows that NPNa single crystal was optically transparent in the entire visible and near IR region with lower cut-off wavelength 492nm. The FTIR and Micro-Raman spectrum confirmed the functional group presence in the compound. TG-DTA and DSC studies reveal that the NPNa crystals have good thermal stabilities. The SHG efficiency of the grown NPNa single crystal was 1.2 times greater than that of KTP crystals. Owing to its transparency, molecular strength and noncentrosymmetric structure, NPNa crystal is considered as a promising material for NLO applications.

Reference

1. Hisahi Minemoto, Yusuke Ozaki, Nobuo Sonoda, *J. Appl. phys*. 76 (1994) 3975-3980.
2. S. Brahadeeswaran, V. Venkata-ramanan, J. Sherwood and H. L. Bhat, *J. Mater. Chem*. 8(3) (1998) 613-618
3. S. Brahadeeswaran, V. Venkata-ramanan, H. L. Bhat, *J. cryst. Growth* 205 (1999) 548-583.
4. B. Milton Boaz, A. Leo Rajesh, S. Xavier Jesu Raja, S. Jerome Das, *J. Cryst. Growth* 262 (2004) 531-535.
5. B. Milton Boaz, M. Palanichamy, Babu Varghese, C. Justin Raj, S. Jerome Das, *Mater. Res. Bull*. 43 (2008) 3587-3595.
6. B. Milton Boaz, S. Jerome Das, *J. Cryst. Growth* 279 (2005) 383-389.
7. B. Milton Boaz, J. Mary Linet, Babu Varghese, M. Palanichamy, S. Jerome Das, *J. Cryst. Growth* 280 (2005) 448-454.
8. C.Vesta, R. Uthrakumar, C. Justin Raj, A. Jonie Varjula, J.Mary Linet, S. Jerome Das, *J. Mater. Sci. Technol*. 23 (2007) 855-859.

9. B. Milton Boaz, S. Mary Navis Priya, J. Mary linet, P. Martin Deva Prasanth, S. Jerome Das, *Opt. Mater*. 29 (2007) 827-832.
10. S. Cimitan, Stefania Albonetti, L. Forni, F. Peri and Dario Lazzari, *J. Colloid & interface science* 329, (2009) 73-80.
11. S. Dinakaran, S. Jerome Das, *J. Cryst. Growth* 310 (2008) 410-413.
12. M. Jose, B. Sridhar, G. Bhagavannarayana, K. Sugandhi, R. Uthrakumar, C. Justin Raj, D. Tamilvendhan, S. Jerome Das, *J. Cryst. Growth* 312 (2010) 793-799.
13. M. Jose, R. Uthrakumar, A. Jeya Rajendran, S. Jerome Das, *Spectrochim. Acta*, Part A 86 (2012) 495-499.
14. V. Subhashini, S. Ponnusamy, C. Muthamizhchelvan, B. Dhana-lakshmi, *Opt. Mater*. 35 (2013) 1327-1334.
15. Jonie Varjula, A. Ramanand, S. Jerome Das, *Mater. Res. Bull*. 43 (2008) 431-436.
16. R. Uthrakumar, C. Vesta, M. Jose, K. Sugandhi, S. Krishnan, S. Jerome Das, *Physica* B 405 (2010) 3371-3375.
17. H. D. Lutz, W. Eckers, G. Schneider and H. Haeuseler, *Spectrochim. Acta* 37A (1981) 561-567.
18. S.K. Kurtz, T.T. Perry, *J. Appl. Phys.* 39 (1968) 3798-3813.